XIII International Conference on Computational Plasticity. Fundamentals and Applications
COMPLAS XIII
E. Oñate, D.R.J. Owen, D. Peric and M. Chiumenti (Eds)

FINITE ELEMENT MODELLING OF COLD PILGERING OF TUBES

YAĞIZ AZİZOĞLU[*+], MATTIAS GÄRDSBACK[†], BENGT SJÖBERG[†] AND LARS-ERIK LINDGREN[+]

[*] Dalarna University
Sandbacka Park
SE - 811 32 Sandviken, Sweden
email: yaz@du.se

[†] Sandvik Materials Technology
R&D
SE - 811 81 Sandviken, Sweden
email: mattias.gardsback@sandvik.com

[+] Luleå University of Technology
Department of Engineering Sciences and Mathematics
SE - 971 87 Luleå, Sweden
email: lel@ltu.se

Key words: Cold pilgering, cold forming, seamless tubes, finite element analysis, thermo-mechanical analysis, Johnson-Cook, von Mises plasticity.

Abstract. Cold pilgering is a cold forming process used during manufacturing of seamless tubes. The tube with a mandrel inside is fed forward and rotated in stepwise increments, while the roll stand moves back and forth. The total plastic deformation of the tube is such that the cross-sectional area of the tube decreases and the length of the tube increases during the process. However, this is performed in many small incremental steps, where the direction of deformation in a material point changes at each stroke. Most published models of cold pilgering use simplified material models. In reality, the flow stress is dependent on temperature, strain rate, strain history and microstructure. In this work, temperature and strain rate distributions are computed, using a 3D thermo-mechanical FE model, and the influence of temperature and strain rate on the rolling force is investigated. The Johnson-Cook model is employed to describe the flow stress using isotropic hardening. The results show that strain rate and temperature have a significant influence on the roll separation force.

1 INTRODUCTION

Cold pilgering is a cold forming process used to manufacture seamless tubes which for some materials enables area reductions more than 90%. During the process, the tube is compressed between a mandrel on the inside and two rolls on the outside, which are oscillating forward and backward. Before each forward and/or backward stroke, the tube is fed forward and turned. As a consequence, the tube is deformed in many small strain increments in different directions. The deformation is intricate because of the large plastic

deformation, strain rates up to about 100 s^{-1} and with frequent changes of strain direction. The plastic deformation and friction generate a significant amount of heat leading to temperatures up to 300°C despite use of a coolant [1].

Knowledge of the influence of the process parameters is required to obtain specified properties of the tube. The current work is part of a project aiming to develop validated models for the process in order to support design of a robust process. The influence of the flow stress model on the rolling force is investigated in the present paper. A 3D thermo-mechanical FE model of the cold pilgering process is developed. The Johnson-Cook model is used to describe the flow stress accounting for temperature, strain rate and strain path dependency.

2 BACKGROUND

The estimation of roll separation force is required for pilger mill design and to determine limits for tube dimensions or process parameters. To calculate this force accurately a reliable flow stress model is required. Since the 1950s, several models have been published to investigate the roll separation force. In 1954, Siebel and Neumann used an axisymmetric 2D analytic approach to estimate the rolling force without considering the oval shape of the roll grooves [2]. This model was used for many years in the industry to design rolls and mandrels. Two decades later, Yoshida *et al*. performed experiments to measure the roll separation force, reaction forces, contact pressure, length of the contact arc and the strain distribution [3]. Pressure-measuring pins were buried in the groove surface to measure the rolling pressure, from which the contact zone was calculated by considering the load-sensing time. They showed that the model by Neumann and Siebel overestimated the roll separation force. Additionally, the roll stand was stopped randomly during the process, and the strain was measured by using a grid on the tube surface. By gathering the measured parameters, an improved model, which required experimental data, was proposed for the cold pilgering of a copper tube.

In 1984, Furugen and Hayashi presented a 3D analytical model for the cold pilgering process [4]. The tube deformation was modeled as a series of increments, where a material point was traced from the beginning to the end of the process. The cross-section of the tube was divided into a groove and a flange part to model the ovalisation. The roll separation force was calculated as the sum of the radial stress values times the estimated contact area. Calculated and experimental values showed good agreement. This model was used together with experiments by Abe and Furugen to investigate the workability of seamless tubes during cold pilgering for materials with different deformability and for different process conditions [5,6]. Osika and Libura created 2D and 3D analytical models and simulated one stroke of the process to examine the rolling pressure and the axial force [7]. In this work, an isotropic linear hardening model was used. Their simulation results showed good agreement with the experimental results. Huml *et al*. developed an analytical 2D axisymmetric model where the mandrel and groove shapes were given as analytical expressions. They divided the material into four zones in the axial direction [8,9]. In zone one, the material has already been rolled down. In zone two, the material is in contact with both the roll pair and the mandrel (forging zone). In zone three, the material is in contact with only the roll-pair (squeezing zone), and in zone four, the material is not yet hit by the roll pair. Strain increments and strain were

computed by using the plastic zone geometry to estimate the deformation of a thin slab of material during the process. The main novelty of their work was the use of a flow stress model, which takes into account the influence of strain softening due to multidirectional deformation, and a temperature model, which takes into account plastic deformation, friction, lubrication and cooling. The authors concluded that the final yield stress of the pilgered tube is strongly dependent on temperature and that multi-axial loading must be taken into account.

In 2002, Davies *et al* studied the development of an anisotropic yield surface during cold pilgering of a titanium alloy [10], by combining finite element analysis (FEA) and measurements of the yield strength in the axial and tangential directions. A 2D FE model of the cross-sections at four locations during the process was employed to compute the plastic strain, which was divided into primary strain, to decrease the cross-section and elongate the tube, and redundant strains, due to ovalisation. The assumption was then made that the primary strain increased the yield strength in one direction and the redundant strain increased the yield strength in another direction.

The first 3D FE model was used by Mulot *et al*. in 1996 [11]. It was used to analyse one forward stroke of the cold pilgering process for Zircaloy-4. They compared the rolling force computed with FEA and a slab method. Even though one stroke is not sufficient for this cyclic process, they demonstrated that FEA is required to capture the completely different stress and strain states in the flange and bottom of the groove. Montmitonnet *et al*. simulated three strokes and found that the stress and rolling forces were almost identical in all strokes in the unrealistic case where a non-work-hardening material was used [12]. A development of the model accounting for work hardening was presented in 2006 by Lodej *et al*. [13]. They used a post-processing procedure for results from a 3D FE model of cold pilgering and estimated strain and stress trajectory of a material point based on the results from a single stroke. The aim of this work was to decrease the calculation cost.

Harada *et al*. used a 2D axisymmetric generalised plane strain model for the simulation of cold pilgering of a zircaloy tube [14]. The material was assumed to have viscoplastic behaviour when exposed to a loading and elastic unloading afterwards. They examined the effect of tube spring-back on the roll separation force and found better agreement with the experiment when the spring-back is considered. Frolov *et al.* investigated the heat conditions of the cold pilger rolling. They used pre-heated mandrels at various temperature and examined the influence on the vertical component of rolling force [15].

In 2012, Vanegas-Márquez *et al*. used a simple Chaboche-type constitutive model to capture the experimental trend of an ODS steel subjected to multi-axial strain cycling similar to the cold pilgering process [16]. The plasticity model accounted for mixed isotropic-kinematic hardening and used the von Mises yield criterion. The model parameters were identified by compression-compression cycling tests and a semi-automated inverse analysis methodology. Anisotropic behavior of an ODS steel due to crystallographic texture and a strongly elongated grain morphology in the rolling direction was included in the model by Vanegas *et al*. [17]. Hill's quadratic plastic anisotropy was used and identification of the parameters was obtained by compression tests of cylindrical specimens cut in three different directions (longitudinal, radial and ortho-radial).

The physical modelling of a new cold pilgering process was performed in laboratory environment with the aim to improve the classic cold pilgering operation by Osika *et al* [18]. They printed grids on the surface of an aluminum tube and measured the deformation in the

working zone. Computations using both the finite difference method (FDM) and FEM were used to determine the strain field. However, the inner surface of the tube was not taken into account so the strain field cannot be considered as 3D. Recently, Pociecha *et al*. [19] used the same cold pilgering setup for both experimental and numerical analyses. Photogrammetric methods were used to measure the deformation on the aluminum tube surface by printed grids and the thickness was measured by non-destructive testing after each stroke. The flow stress data used in the simulation were obtained from a tensile test. No temperature, strain rate or multi-axial strain recovery were accounted for in the model. Still, the calculated deformation and metal pressure force on the rollers agreed well with experimental values.

3 MODELLING

3.1 FE model

A 3D thermo-mechanical FE model of the cold pilgering process is developed in the commercial software MSC Marc and Mentat. The geometry is given in Figure 3.1. The pilgered cone consists of the working part, the sizing section and the opening part. The length of the working part is normalised to one. The rolls have a conical shape with oval groove and the mandrel has a conical shape in the working part. The arc length of the working part of the rolls is equal to the length of the working part of the mandrel. In the sizing section, the shape of the roll grooves and the mandrel diameter are constant. In the opening part, the tube is not in contact with the tools. Instead, the tube is feed forward and turned by an imaginary steering plate. The rolls are rolling back and forth during the process. In this study, 40 strokes (forward + backward) were applied. During a stroke, the rolls press the tube towards the mandrel.

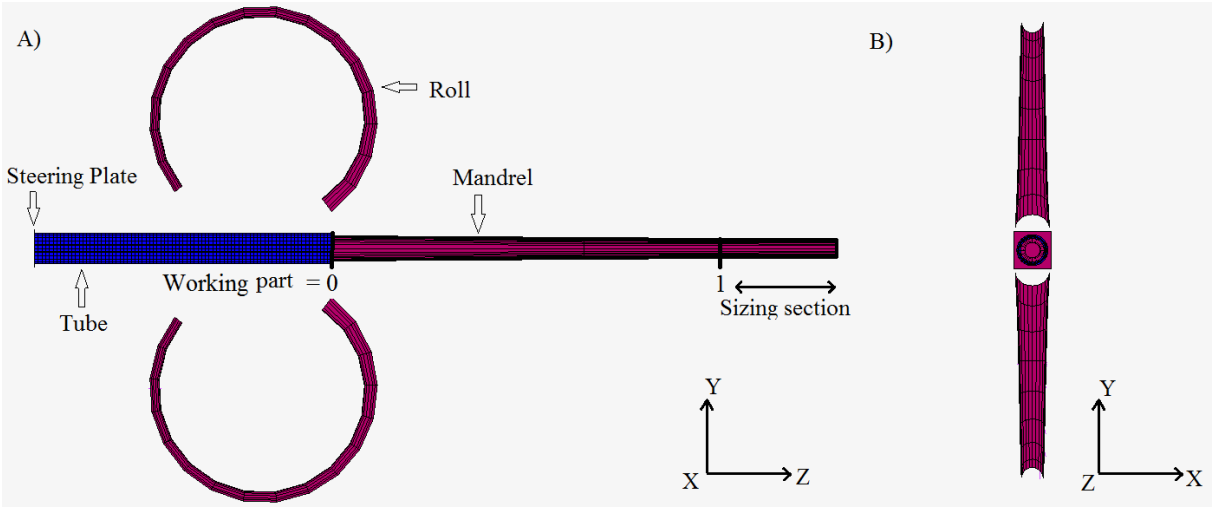

Figure 3.1: The geometry of the FE model.

The following simplifications have been made in the model:

- The tools and the roll stand are assumed to be rigid.

- Isotropic hardening of the material is assumed.
- All plastic dissipated energy and work done by friction is converted to heat.
- Coulomb friction, with a friction constant 0.2, is assumed between both work piece and rolls and work piece and mandrel.
- Heat convection to the environment is used to mimic coolant.
- The tube is cooled continuously at the surface, $A_{surface}$, with a constant heat transfer coefficient, h. The lost heat flux per unit area is:

$$q=h(T_{tube\ surface}-T_{sink}) \tag{3.1}$$

The model is solved using the finite element code MSC.Marc, version 2013.r1, with implicit time stepping. The nonlinear system of equations was solved by in an incremental, iterative procedure using the full Newton-Raphson method. The reference case required only a mechanical analysis as no temperature changes were accounted for, Coupled thermo-mechanical analyses were used for the other cases.

3.2 Temperature model

Lubrication is important for both the surface quality of the tube and the tool life [1,20]. The lubrication oil shows optimal performance in a certain temperature range and above 300 ℃ the oil may get burnt. Oil jet cooling is a method to decrease friction and the tube surface temperature. In the simulation, the effects of the temperature model are:

- There is more heating in the beginning of the working cone, since there is more plastic deformation.
- The oil cooling jet is not directly included in the model since this is fairly complex process [1,20] and therefore the heat transfer coefficient is fit so that the computed temperature corresponds to a measured temperature at the outside of the tube after the cold pilgering.

3.3 Material model

Employing the correct constitutive model is important for the model. The non-proportional and multi-axial loading of this process makes evaluation of the yield surface quite difficult. In this work, a rather simple model was used: von-Mises plasticity with isotropic hardening. The Johnson-Cook model is employed to describe the evolution of the flow stress (Eq. 3.2). In the equation: ε_p is the equivalent plastic strain, $\dot{\varepsilon}_p$ is the plastic strain-rate, and A, B, C, n, m are material constants. $\dot{\varepsilon}_p^*$ and T^* are the normalised strain rate and the normalised temperature respectively, given in Eq. 3.3. In this equation T is the temperature variable, T_0 is the reference temperature, $\dot{\varepsilon}_p$ is the plastic strain rate variable and $\dot{\varepsilon}_{p0}$ is the effective plastic strain rate of the quasi-static test, which is used to find the parameters; A, B and n.

$$\sigma_y(\varepsilon_p,\dot{\varepsilon}_p,T)=[A+B(\varepsilon_p)^n][1+Cln(\dot{\varepsilon}_p^*)][1-(T^*)^m] \tag{3.2}$$

$$\dot{\varepsilon}_p^*=\frac{\dot{\varepsilon}_p}{\dot{\varepsilon}_{p0}} \quad \text{and} \quad T^*=\frac{(T-T_0)}{(T_m-T_0)} \tag{3.3}$$

The parameters in this model were obtained from the compression tests of the used stainless steel. The Johnson-Cook parameters are given in Table 3.1 and the other material data are given in Table 3.2.

Table 3.1: Johnson-Cook model parameters

A	2.2397e+07 Pa
B	1.3687e+09 Pa
n	0.4488
C	0.0162
m	0.7708
T_0	20 ℃
T_m	1385℃
$\dot{\varepsilon}_{p0}$	0.01 s^{-1}

Table 3.2: Material data

Temperature (℃)	20	150	300
Young`s Modulus*(GPa)	195	195	195
Poisson`s Ratio	0.29	0.29	0.29
Mass Density (kg/m^3)	8000	8000	8000
Thermal Conductivity (W/m℃)	11	13	16
Specific Heat (J/kg℃)	460	495	525
Convective heat transfer coefficient (W/m^2℃)	8300	8300	8300

The Johnson-Cook model is plotted for various strain rate and temperature values in Figure 3.2.

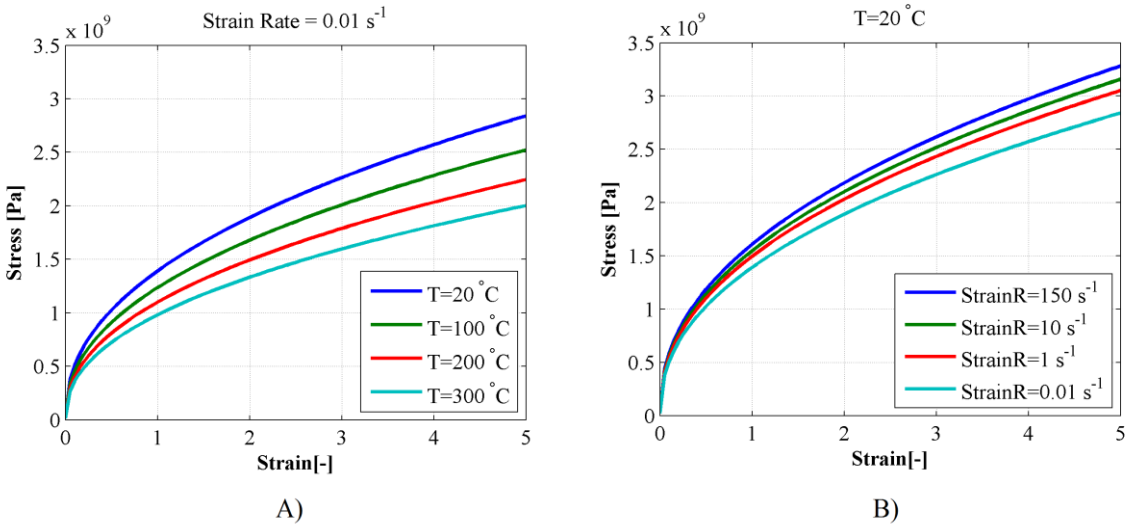

Figure 3.2: Flow stress curves for A) various temperatures B) various strain rates.

3.4 Process parameters

Feed step, rotation angle, feed/rotation distribution and stroke rate are process parameters that can be used to control the product properties of the final tube. They also have a great influence on the process temperature. The area reduction and the final tube diameters are given in Table 3.3. Stainless steel can tolerate large area reductions due to its ductility. A large area reduction give rise to a high temperature increase in the material.

Table 3.3: Process data

Cross-section area reduction (%)	70
Final tube, outer diameter (mm)	25.4
Final tube, thickness (mm)	2.4

4 RESULTS AND DISCUSSION

Three different models were considered to examine the influence of temperature, strain rate and strain softening due to multi-axial loading. In the first model flow stress corresponding to a temperature of 20 °C and a strain rate of 0.01 s-1 was used. This model is named “Reference” in the following text. The second model accounted for heat generation due to plastic deformation and friction. The Johnson-Cook model was used to model the flow stress as a function of temperature and strain rate during the process as described earlier. This model is named “Heat”. In the third model, the constants A and B in the Johnson-Cook model were decreased by 10% and the other constants were identical to the ones in the second model. This model represents a material with lower flow stress according to the strain path in [8]. It is named “Heat & Low”.

In Figure 4.1, equivalent plastic strain rates at four angular positions of a tube cross-section, moving from the beginning to the end of the working cone, are shown. This figure was obtained from the reference model. The angular positions are represented by their clock position, which are defined in Figure 4.2. Each peak corresponds to a stroke. According to Figure 4.1, the maximum strain rate is obtained near position 0.6 of the working cone. Nodes at different angular positions have different strain rate values within a stroke, due to ovalisation of the cross-section.

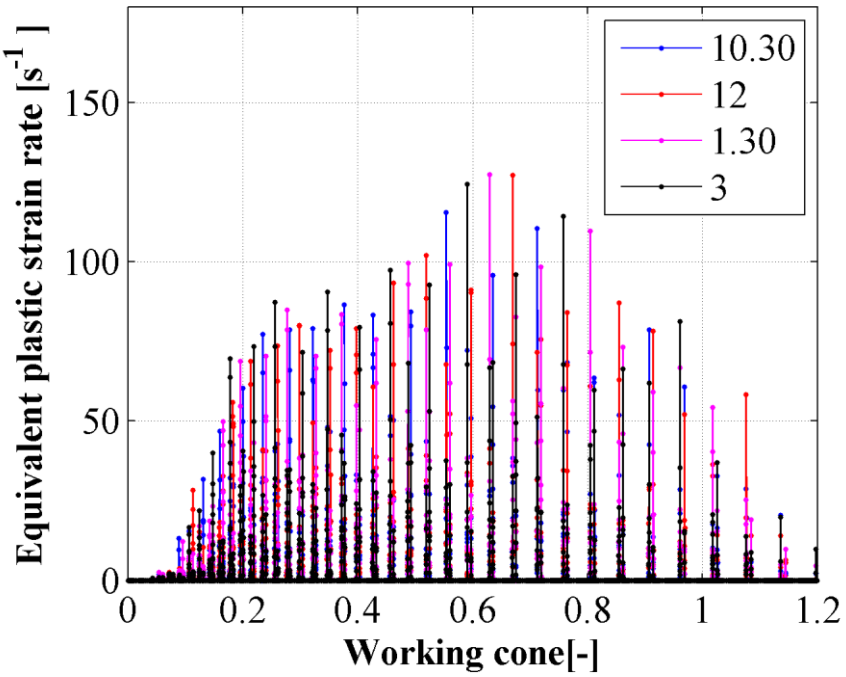

Figure 4.1: Strain rate versus the position of cross-section over the pilger stroke.

Figure 4.2 shows the plastic strain rate in the compression zone for a cross-section of a pilgered tube. The two zones that are in contact with both the rolls and the mandrel, from 10.30 to 1.30 in the upper half and analogously in the lower part, are heavily deformed while the deformation is very small in the rest of the cross-section. This is in good agreement with the 2D model by Furugen and Hayashi [4]. The outside of the tube in the compressed part is also deformed more than the inside of the tube, which cannot be explained by neither 2D axisymmetric models [2,8,9] nor 2D models of the cross-section [7,10,14]. The reason for the greater deformation on the outside is the velocity of the rolls on the outside compared to the stationary mandrel on the inside. The asymmetric deformation shows the need for a finite element model.

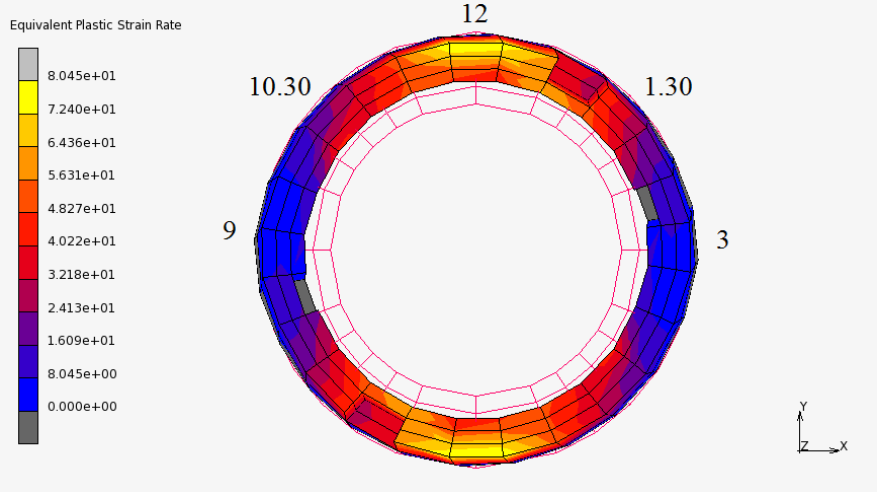

Figure 4.2: Equivalent plastic strain rate in a selected tube cross-section.

Figure 4.3 shows the temperature distribution on the tube surface after 40 forward and backward strokes. In the figure, the highest temperature is obtained in the middle of the working cone even though there is more heating in the beginning of working cone. The reason is that plastic deformation heat is accumulated during the process and the heating is faster than the cooling until the point of the highest temperature. After that the plastic deformation decreases, but the tube is still cooled.

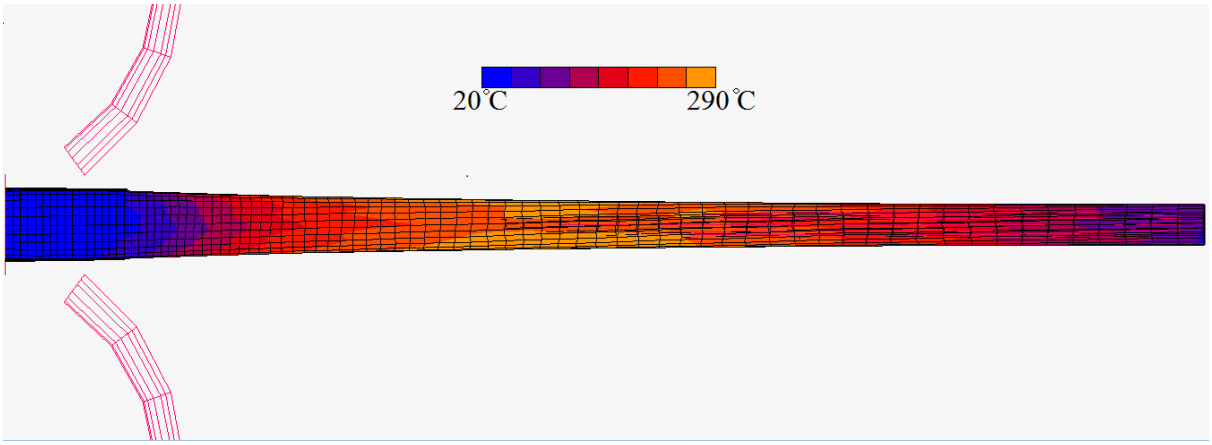

Figure 4.3: FE model of the cold pilgered tube at the end of process.

The roll separation force variation over the working cone during the last forward stroke is shown in Figure 4.4 for the different cases. The roll separation forces show similar trends as in the papers by Furugen and Hayashi [4] and Yoshida et al. [3]. There is a fairly large influence of temperature and strain rate on the roll separation force. The roll separation force decreases most around 0.5 of the working cone. This is due to that the temperature has the highest value near this position. The equivalent strain rate is also fairly high in this region, but thermal softening dominates over the strain hardening due to high strain rate. The multi-low

case has even lower roll separation force. The results show that it is necessary to account for temperature, strain rate and lower flow softening according to estimate the correct roll separation force.

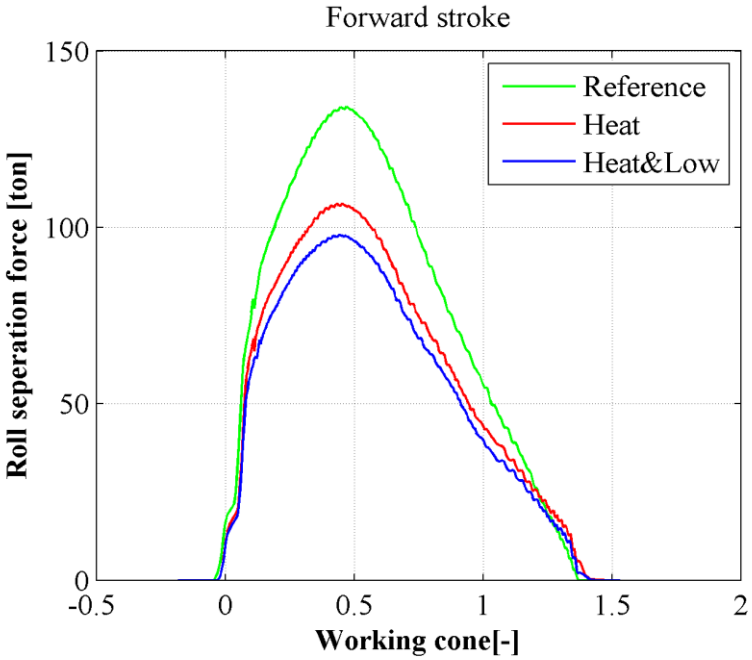

Figure 4.4: Roll separation force over the pilger stroke for three different cases.

5 CONCLUSIONS

It has been found, as expected, that the strain rate and temperature influences on the flow stress have large effect on the roll separation force. Lower roll separation force was obtained once temperature and strain rate dependencies were included in the material model.

It was shown that, nodes at different angular positions have different strain rate values within the same stroke. This cannot be captured by 2D models of the process. It is necessary to use a full 3D model describing the asymmetric deformation of the process.

REFERENCES

[1] Carscallen, W.E., Jeswiet, J., Oosthuizen, P.H. *Optimization of a Cooling System: the Cooling of Pilgered Seamless Tubes*. CIRP Annals - Manufacturing Technology, Vol. 43, (1994).

[2] Siebel, E. and Neumann, F.W. *Das Kaltpilgern von Rohren - versuchergebniße und Untersuchungen über dem Walzvorgang.* Stahl und Eisen, Vol. 74, (1954).

[3] Yoshida, H., Matsui T., Otani, T., Mandai, K. *Experimental investigation of the cold pilgering of copper tubes.* Annals of the CIRP, Vol 24, (1975).

[4] Furugen, M. and Hayashi, C. *Application of the theory of plasticity to the cold pilgering of tubes.* J. Mech. Work. Tech., Vol. 10, (1984).

[5] Abe, H. and Furugen, M. *Method of Evaluating Workability in Cold Pilgering of Zirconium Alloy Tube.* Materials Transaction, Vol 51, (2010).

[6] Abe, H. and Furugen, M. *Method of Evaluating Workability in Cold Pilgering*. Journal of Materials Processing Technology, Vol. 212, (2012).
[7] Osika, J. and Libura, W. *Mathematical model of tube cold rolling in pilger mill.* Journal of Materials Processing Technology, Vol. 34, (1992).
[8] Huml, P. and Fogelholm, R. *Optimization of Cold Rolling of Precision Tubes*. CIRP, Vol 42, (1993).
[9] Huml, P. and Fogelholma, R. *Simulation model of cold pilgering.* J. Mater. Process. Technol., Vol 42, (1994).
[10] Davies, R. W. and Khaleel A. M. *Anisotropic Yield Locus Evaluation During Cold Pilgering of Titanium Alloy Tubing*, J. Eng. Mater. Technol. Vol 124, (2002).
[11] Mulot, S., Hacquin, A., Montmitonnet, P. and Aubin, J.-L. *A fully 3D finite element simulation of cold pilgering.* J. of Materials Processing Technology, Vol 60, (1996).
[12] Montmitonnet, P., Logé, R., Hamery, M., Chastel, Y., Doudoux, J.-L., and Aubin, J.-L. *3D elastic-plastic finite element simulation of cold pilgering of zircaloy tubes.* J. Mat. Proc. Tech. Vol 125-126, (2002).
[13] Lodej, B., Niang, K., Montmitonnet, P., Aubin, J.-L., *Accelerated 3D FEM computation of the mechanical history of the metal deformation in cold pilgering of tubes*, Journal of Materials Processing Technology, Vol 177, (2006).
[14] Harada, M., Honda, A. and Toyoshima, S. *Simulation of Cold Pilgering Process by a Generalized Plane Strain FEM*. J. of ASTM International, Vol 2, (2005).
[15] Frolov, Ya. V., Mamuzić, I., Danchenko, V. N. *The Heat Conditions of the Cold Pilger Rolling*, Metallurgy, Vol. 45 (June 2006)
[16] Vanegas-Márquez, E., Mocellin, K., Toualbi, L., Carlan, Y. de, Logé, R.E., *A simple approach for the modeling of an ODS steel mechanical behavior in pilgering conditions.* Journal of Nuclear Materials, Vol. 420, (2012).
[17] Vanegas, E., Mocellin, K. and Logé, R. *Identification of cyclic and anisotropic behaviour of ODS steels tubes.* Procedia Engineering, Vol. 10, (2011).
[18] Osika, P., Palkowski, H., Świątkowski, K., Pociecha, D., Kula, A. *Analysis of Material Deformation during the New Cold Tube Rolling Process Realized on the New Generation of Pilger Mills*. Archives of Metallurgy and Materials, Vol. 54, (2009).
[19] Pociecha, D., Boryczko, B., Osiko, J., and Mroczkowski, M. *Analysis of tube deformation process in a new pilger cold rolling process.* Arc. Civ. Mech. Engng, Vol 14, (2014).
[20] Abe, H., Nomura, T. and Kubota, Y. *Lubrication of tube in cold pilgering*, Journal of Materials Processing Technology, Vol 214, (2014).